Silencing of lncRNA TFAP2A-AS1 attenuates the development of acute coronary syndrome by inhibiting TFAP2A expression

SHIWEI HUANG[1], FANLU GUAN[1], FANHAO YE[1], BOZHI YE[2], SISI HAN[1] and HAO CHEN[1]

[1]Department of Cardiovascular Medicine, Wenzhou People's Hospital, Wenzhou, Zhejiang 325000, P.R. China; [2]Department of Cardiovascular Medicine, The First Affiliated Hospital of Wenzhou Medical University, Wenzhou, Zhejiang 325000, P.R. China

Received June 17, 2024; Accepted July 21, 2025

DOI: 10.3892/br.2025.2093

Abstract. Acute coronary syndrome (ACS), the acute manifestation of ischemic heart disease, remains a major cause of morbidity and mortality worldwide. The present study aimed to elucidate the preliminarily biological role and underlying mechanism of the long non-coding RNA (lncRNA) transcription factor AP-2α (TFAP2A)-AS1 in ACS. The viability, apoptosis, invasion, and migration of human coronary artery endothelial cells (HCAECs) were assessed using Cell Counting Kit-8, flow cytometric, Transwell, and wound healing assays. In addition, reverse transcription-quantitative PCR was performed to examine the expression levels of TFAP2A-AS1 and TFAP2A. Western blotting was performed to determine the protein level of TFAP2A. Furthermore, a mouse model of ACS was established to investigate the effects of TFAP2A-AS1 and TFAP2A on blood lipid levels. Histological changes were evaluated through hematoxylin and eosin staining. The results revealed high levels of TFAP2A-AS1 and TFAP2A expression in patients with ACS and in mouse models. In HCAECs, knockdown of TFAP2A-AS1 resulted in decreased TFAP2A expression, whereas silencing of TFAP2A did not affect the expression of TFAP2A-AS1. Interference with either TFAP2A-AS1 or TFAP2A in HCAECs led to suppressed cell viability, invasion, and migration, as well as an increased apoptosis rate. Furthermore, it was demonstrated that the absence of both TFAP2A-AS1 and TFAP2A reduced blood lipid levels and improved myocardial injury in a mouse model of ACS. In conclusion, groundbreaking findings revealed that the suppression of TFAP2A-AS1 could effectively mitigate the progression of ACS by reducing the expression of TFAP2A. This finding not only offers crucial insight into the pathogenesis of ACS but also provides a solid theoretical foundation for the development of novel therapeutic interventions in clinical settings.

Correspondence to: Dr Hao Chen, Department of Cardiovascular Medicine, Wenzhou People's Hospital, 299 Gu'an Road, Wenzhou, Zhejiang 325000, P.R. China
E-mail: leochenhao@163.com

Abbreviations: lncRNA, long non-coding RNA; ACS, acute coronary syndrome; HCAECs, human coronary artery endothelial cells; CVDs, cardiovascular diseases; STEMI, ST-segment elevation myocardial infarction; NSTEMI, non-ST-segment elevation myocardial infarction; UA, unstable angina pectoris; GC, gastric cancer; BC, breast cancer; NSCLC, non-small cell lung cancer; OSCC, oral squamous cell carcinoma; EBM-2, endothelial basal medium 2; FBS, fetal bovine serum; TC, total cholesterol; HDL-C, high-density lipoprotein-cholesterol; LDL-C, low-density lipoprotein-cholesterol

Key words: acute coronary syndrome, lncRNA, TFAP2A-AS1, transcription factor AP-2α

Introduction

Cardiovascular diseases (CVDs) are responsible for the majority of illnesses and deaths worldwide, accounting for 49% of female and 40% of male deaths (1). Acute coronary syndrome (ACS), a type of CVD, encompasses acute ST-segment elevation myocardial infarction (STEMI), acute non-STEMI ST-segment elevation myocardial infarction (NSTEMI), and unstable angina pectoris (UA). These conditions arise from the rupture or invasion of plaques in coronary arteries affected by atherosclerosis (2,3). ACS often serves as a significant risk factor for acute heart failure (4). Despite advancements in treatment options, such as coronary revascularization, antithrombotic agents, and anticoagulants, approximately one-fifth of patients with ACS experience recurrent adverse cardiovascular events within 3 years following the initial diagnosis (5,6). Therefore, a deeper understanding of the molecular mechanisms underlying ACS is crucial for improving patient outcomes.

Long non-coding RNAs (lncRNAs) are a type of ncRNA consisting of over 200 nucleotides that cannot encode proteins. They have been scientifically proven to influence various biological processes, including epigenetics, transcription, and post-transcriptional regulation in living organisms (7). Several studies have highlighted the involvement of numerous lncRNAs in ACS diagnosis and development of ACS. Chen *et al* (8) conducted a microarray analysis of serum samples obtained from individuals with ACS and identified 353 dysregulated lncRNAs. Subsequent investigations revealed that the modulation of arachidonate 15-lipoxygenase expression by a specific lncRNA ENST00000538705.1 could expedite the progression of ACS (8). Additionally, Barbalata *et al* (9)

found an association between two distinct lncRNAs (LIPCAR and MALAT1) and hyperglycemia in patients with UA, identifying them as reliable prognostic indicators of adverse outcomes in patients with STEMI (9). Another study revealed a negative association between increased levels of lncRNA PELATON and ACS prognosis (10). Notably, transcription factor AP-2α (TFAP2A)-AS1 is a relatively understudied lncRNA located on chromosome 6q24.3. Current research on lncRNA TFAP2A-AS1 has primarily focused on its impact on the pathogenesis and progression of various human cancers. For instance, elevated expression of TFAP2A-AS1 has been associated with improved prognosis in gastric cancer (GC) and breast cancer (BC), whereas overexpression of TFAP2A-AS1 in GC and BC cells suppressed cell proliferation, migration, and invasion (11,12). Conversely, TFAP2A-AS1 was shown to be highly expressed in non-small cell lung cancer (NSCLC) and oral squamous cell carcinoma (OSCC); however, its absence inhibited tumor development (13,14). Nevertheless, the precise biological role and mechanism of action of TFAP2A-AS1 in ACS remain poorly understood.

The aim of the present study was to explore the mechanism of action of TFAP2A-AS1 in the pathogenesis of ACS and to identify potential molecular targets for therapeutic intervention in patients with ACS.

Materials and methods

Patients and diagnostic criteria. The present research adhered to the principles outlined in the Declaration of Helsinki and received approval (approval ID: KY-2021053) from the Ethics Committee of Wenzhou People's Hospital (Wenzhou, China). From September 2021 to October 2022, a total of 5 patients diagnosed with ACS were admitted to Wenzhou People's Hospital. Concurrently, 5 healthy individuals of comparable age were recruited to serve as controls. The diagnostic criteria for ACS included confirmed stenosis (at least one major coronary artery ≥50%) through coronary angiography, and/or meeting the acute myocardial infarction criteria (typical clinical symptoms, elevated cardiac enzyme levels, and representative electrocardiography findings). The inclusion criteria were as follows: i) Meeting the diagnostic criteria; ii) age between 35-75 years; and iii) providing informed consent. The exclusion criteria were as follows: i) The presence of comorbid conditions such as cardiomyopathy, valvular heart disease, severe arrhythmia, heart failure or other concurrent ailments; ii) challenges in data collection due to religious or language barriers; and iii) being pregnant or breastfeeding. Venous blood samples (5 ml) were collected from both patients with ACS and healthy controls. The samples were then centrifuged at 3,000 x g at a temperature of 4˚C for a duration of 5 min. Following centrifugation, the samples were stored at -80˚C for subsequent experiments. The clinicopathological factors of healthy controls and patients with ACS are summarized in Table I.

Reagents. Human primary coronary artery endothelial cells (HCAECs), mouse coronary artery endothelial cells (MCAECs) and 293 cells were sourced from Pricella Biotechnology Co., Ltd. The utilization of primary cells was approved (approval ID: KZ-20240521) by the Ethics Committee of Wenzhou People's Hospital. Endothelial basal medium 2 (EBM-2) and fetal bovine serum (FBS) were obtained from Lonza Group, Ltd. CCK-8 solution was provided by Abbkine Scientific Co., Ltd. BD Biosciences provided the Matrigel. Genomeditech (Shanghai) Co., Ltd. Synthesized TFAP2A-AS1 small interfering (si)RNA1/2/3, TFAP2A siRNA1/2/3, lentiviral vectors integrated with TFAP2A-AS1 shorth hairpin (sh)RNA/TFAP2A shRNA, and the corresponding negative controls (NC siRNA or NC shRNA). Vazyme Biotech Co., Ltd. supplied an Annexin V-FITC/PI Apoptosis Detection kit. Beyotime Institute of Biotechnology provided the hematoxylin and eosin (H&E) staining kit, the RIPA lysis buffer, the enhanced chemiluminescence (ECL) kit and the bicinchonic acid (BCA) kit. Thermo Fisher Scientific, Inc. provided the Lipofectamine RNAiMAX transfection agent and Pierce Magnetic RNA-Protein Pull-Down kit (cat. no. 20164). Beijing Solarbio Science & Technology Co., Ltd. supplied the Total cholesterol (TC) Content Assay Kit (cat. no. BC1980). Nanjing Jiancheng Bioengineering Institute provided the high-density lipoprotein-cholesterol (HDL-C) assay kit (cat. no. A112-1-1) and low-density lipoprotein-cholesterol (LDL-C) assay kit (cat. no. A113-1-1). Takara Biotechnology Co., Ltd. supplied the MiniBEST Universal RNA Extraction kit (cat. no. 9767). Invitrogen; Thermo Fisher Scientific, Inc. supplied the PrimeScript RT reagent and SYBR Green Premix for the experiment. Primary antibodies TFAP2A (cat. no. 13019-3-AP), IgG control (cat. no. 30000-0-AP) and GAPDH (cat. no. 60004-1-Ig) were purchased from Proteintech Group, Inc., along with horseradish peroxidase (HRP)-conjugated secondary antibodies (cat. no. SA00001-2). The Magna RIP RNA-Binding Protein Immunoprecipitation kit (cat. no. 17-700) was obtained from MilliporeSigma.

Cell culture. The HCAECs were cultured in EBM-2 supplemented with 15% FBS, under conditions of 5% CO_2 and a temperature of 37˚C. For functional experiments, cells in the phase of logarithmic growth were collected.

Cell transfection. Cell transfection was performed in strict accordance with the protocols of Lipofectamine RNAiMAX transfection reagent. In brief, HCAECs were individually transfected with 50 nM of TFAP2A-AS1 siRNA1/2/3 (TFAP2A-AS1 siRNA1 forward, 5'-UGCUAAUGAGGCGAUUAGGCU-3' and reverse, 5'-CCUAAUCGCCUCAUUAGCAUA-3'; TFAP2A-AS1 siRNA2 forward, 5'-AUUUCUAAUAAAAUUGCACGG-3' and reverse, 5'-GUGCAAUUUUAUUAGAAAUCA-3'; TFAP2A-AS1 siRNA3 forward, 5'-UGUUUUUAGGCUCAACUUCAG-3' and reverse, 5'-GAAGUUGAGCCUAAAAACAGA-3'); TFAP2A siRNA1/2/3 (TFAP2A siRNA1 forward, 5'-AUUUAAUCCUAUUUUGUCCAG-3' and reverse, 5'-GGACAAAAUAGGAUUAAAUCU-3'; TFAP2A siRNA2 forward, 5'-UUGCAUAUCUGUUUUGUAGCC-3' and reverse, 5'-CUACAAAACAGAUAUGCAAAG-3'; TFAP2A siRNA3 forward, 5'-UGCUUUUGGCGUUGUUGUCCG-3' and reverse, 5'-GACAACAACGCCAAAAGCAGU-3'); and NC siRNA forward, 5'-GAAAUGUUUAGGGCCAGUGCU-3' and reverse, 5'-AGCACUGGCCCUAAACAUUUC-3' for 48 h at 37˚C using Lipofectamine RNAiMAX transfection reagent. Following transfection, cells were collected for subsequent experiments.

Table I. Clinicopathological factors of healthy controls and patients with ACS.

Characteristics	Healthy controls (n=5)	Patients with ACS (n=5)	P-value
Age, years	64.00±3.03	62.40±10.07	0.7425
BMI, kg/m^2	24.66±4.21	25.12±3.28	0.8520
Sex (male/female)	2/3	2/3	N/A
Smoking, (N/total)	2/5	2/5	N/A
Drinking, (N/total)	2/5	2/5	N/A
Hypertension, (N/total)	3/5	3/5	N/A
Cardiac troponin I, μg/l	0.014±0.0001	4.57±0.21	<0.0001

ACS, acute coronary syndrome; BMI, body mass index; N/A, not applicable.

Flow cytometric analysis. The apoptosis of HCAECs was assessed by employing a commercially available Annexin V-FITC/PI Apoptosis Detection kit. Briefly, HCAECs (2x10^5) were suspended in 500 μl of binding buffer, and subsequently stained with PI and Annexin V-FITC (both 5 μl) at 4˚C for 15 min in the absence of light. Following this step, cell apoptosis was evaluated using a FACScan flow cytometer (version 3.0; Becton, Dickinson and Company) and analyzed using BD CellQuest Pro software (version 5.2.1; Becton, Dickinson and Company). Cells were classified as viable cells (lower left quadrant), necrotic cells (upper left quadrant), early apoptotic cells (lower right quadrant) and late apoptotic cells (upper right quadrant). The apoptosis rate was estimated by calculating the total percentages of both early and late apoptotic cells.

CCK-8 assay. HCAECs were cultured in 96-well plates at a density of 3,500 cells per well and incubated for various time intervals (24, 36, 48, and 72 h). Subsequently, each well was supplemented with 10 μl of CCK-8 solution and further incubated for 2 h at 37˚C. Following the addition of 10 μl of stop solution to every well, cell viability was assessed using a microplate reader (DR-3518G; Wuxi Hiwell Diatek Instruments Co., Ltd.), which measured the absorbance at a wavelength of 450 nm.

Transwell assay. The upper chamber of Transwell insert was pre-coated with 50 μl of Matrigel at 37˚C for 30 min, which had been diluted 5-fold in serum-free EBM-2. HCAECs were incubated for 24 h following digestion, after which the culture medium was removed by centrifugation (1,500 x g; at 4˚C for 5 min). Subsequent to washing with PBS, 1x10^5 resuspended cells were seeded into the Transwell chamber and incubated for an additional 24 h. The cells were then fixed with 4% paraformaldehyde at 37˚C for 15 min, washed, and stained with crystal violet at 37˚C for 15 min. The invasive cells were observed under a light microscope (Leica Microsystems GmbH), and images were captured from three randomly selected fields of view.

Wound healing assay. HCAECs were cultured in 6-well plates at a density of 3x10^5 cells per well. Once the cells attained 100% confluence, a scratch was created on the monolayer using a 10 μl pipette tip. Subsequently, HCAECs were incubated in serum-free EBM-2 at 37˚C for 48 h. The widths of the scratches at both 0 h (initial width) and 48 h (final width) were observed using a light microscope (Leica Microsystems GmbH). To assess the migratory abilities of HCAECs, ImageTool software version 3.0 (UTHSCSA, San Antonio, USA) was employed with the following formula: (Initial width-final width)/initial width x100%.

RNA immunoprecipitation (RIP) assay. The Magna RIP RNA-Binding Protein Immunoprecipitation kit was used for RIP assays following the manufacturer's protocol. Briefly, HCAECs were collected and lysed using RIP lysis buffer. For each IP reaction, HCAECs (2x10^7 cells) were resuspended in 1 ml of lysis buffer and incubated on ice for 30 min. The samples were then centrifuged at 14,000 x g for 20 min at 4˚C. Whole-cell extracts were incubated with RIP buffer (at 4˚C for 30 min) containing magnetic beads conjugated to human anti-TFAP2A antibody or the control IgG. The beads were then washed five times with 1 ml wash buffer and centrifuged at 1,000 x g for 1 min at 4˚C between washes. Subsequently, 100 μl of elution buffer was added in the samples to incubate for 10 min at 65˚C. Proteinase K was added to the samples to digest the protein, and the immunoprecipitated RNA was isolated. Purified RNA was used for reverse transcription-quantitative PCR (RT-qPCR) analysis. The expressional level of GAPDH was used as the control.

RNA pull-down assay. The interaction between TFAP2A-AS1 and TFAP2A protein was examined using Pierce Magnetic RNA-Protein Pull-Down kit according to the manufacturer's protocols. Proteins from HCAECs were extracted using lysis buffer (20 mM Tris-HCl, 150 mM NaCl, 1% NP-40, 10% glycerin, 2 mM EDTA, 1 mM PMSF, 1X Protease inhibitor cocktail, and 40 U/ml RNase). For each reaction, HCAECs (5x10^6 cells) were resuspended in 1 ml of lysis buffer and incubated on ice for 60 min. Biotin-labeled TFAP2A-AS1 or antisense RNA was co-incubated with protein extract of HCAECs and Protein G-magnetic beads (40 μl). The generated bead-RNA-Protein compound was collected by low-speed centrifugation (800 x g for 2 min at 4˚C). After being washed with 2X SDS loading buffer, the bead compound was boiled for 10 min in SDS buffer, and the retrieved protein was detected by western blotting with the expressional level of GAPDH as the control.

Table II. Real-time PCR primer synthesis list.

Gene	Sequences
LncRNA TFAP2A-AS1	Forward 5'-GCATCCACGTCCTCTCTCTG-3'
	Reverse 5'-GCAGATTGTGGTACTGGCGA-3'
TFAP2A	Forward 5'-TCCGCTTCACGCTCGATTT-3'
	Reverse 5'-AATCCGTGTCTCCCCCTCTT-3'
GAPDH	Forward 5'-TCAAGAAGGTGGTGAAGCAGG-3'
	Reverse 5'-TCAAAGGTGGAGGAGTGGGT-3'

TFAP2A, transcription factor AP-2α.

Animal grouping and treatment. Animal experiments were conducted in accordance with the Guidelines for the Use of Laboratory Animals and approved by the Ethics Committee of the First Affiliated Hospital of Wenzhou Medical University (approval no. xmsq2022-1230). A total of 24 C57BL/6J mice, weighting 18-22 g and aged 8 to 10 weeks, were procured from Pengsheng Biological Technology Co., Ltd. The ACS mouse model was established in accordance with a previously described protocol (15). C57BL/6J mice were randomly assigned to four groups: Sham group, ACS model + NC shRNA group, ACS model + TFAP2A-AS1 shRNA group, and ACS model + TFAP2A shRNA group. Each group consisted of six mice. Anesthesia was induced through an intraperitoneal injection of pentobarbital sodium at a dose of 50 mg/kg. The limbs of the mice were then secured on a surgical table while maintaining them in a supine position. A thoracotomy was performed to expose the heart, followed by ligation of the anterior descending coronary artery using 6/0 surgical sutures. To prevent infection, each mouse was administered a subcutaneous injection of penicillin at a dose of 50 mg/kg. By contrast, the mice in the sham group underwent only threading without ligation. Successful establishment of the ACS mouse model was confirmed based on significantly elevated ST segment and/or high T wave readings (data not shown). A three-plasmid system, along with 9 μg of lentiviral vectors, was co-transfected into 293 cells using Lipofectamine RNAiMAX transfection agent at room temperature. The ratio of lentiviral plasmid to packaging vector to envelope was maintained at 1:1:1. The lentivirus-containing culture medium was harvested 48 h post-transfection and subsequently used to infect MCAECs (second passage; $5x10^6$ cells per well) with a multiplicity of infection set at 20. Subsequently, 48 h after infection, the cells were subjected to selection using 1 μg/ml puromycin. Prior to surgery, mice in the ACS model + NC shRNA group received an intramyocardial injection containing lentiviral vectors integrated with the NC shRNA sequence (50 μg; 5'-GGCAGGGTG ATGGGCAACATA-3'). By contrast, those in both the ACS model + TFAP2A-AS1 shRNA and ACS model + TFAP2A shRNA groups were administered with lentiviruses carrying either the TFAP2A-AS1 shRNA sequence (5'-GGCTGGTGA AGAACCTGAAGG-3') or the TFAP2A shRNA sequence (5'-GAGTTGCTTGACCCACTTCAA-3'), respectively, via intramyocardial injection (both at a dose of 50 μg). Anesthesia was maintained for 30 min. The humane endpoints were rapid or labored breathing. After a two-week period, euthanasia was conducted on all groups using an overdose of pentobarbital sodium administered via intraperitoneal injection at a dose of 200 mg/kg. Death was confirmed by cardiac and respiratory arrest and a lack of response to tail clamping. Following the confirmation of death, whole blood samples (300 μl; collected from the eyeballs) and heart tissues were collected for further analysis.

RT-qPCR. The extraction of RNA from heart tissues of mice, HCAECs, and serum samples of patients with ACS, was conducted using the MiniBEST Universal RNA Extraction Kit. Subsequently, reverse transcription into cDNA was performed at 45˚C for 45 min using the PrimeScript RT reagent kit. PCR analysis was then conducted in accordance with the SYBR Green Premix protocols on a QuantStudio7 system (Thermo Fisher Scientific, Inc.). The reaction conditions consisted of an initial denaturation step at 95˚C for 2 min, followed by 40 cycles of denaturation at 95˚C for 10 sec, annealing at 60˚C for 30 sec, and extension at 72˚C for 30 sec. The primers used in the present study are listed in Table II. The relative expression levels of TFAP2A-AS1 and TFAP2A were normalized against GAPDH and calculated using the $2^{-\Delta\Delta Cq}$ method (16).

Western blot analysis. The concentration of total proteins was determined in HCAECs or heart tissues by extracting them with RIPA lysis buffer, followed by measurement using a BCA kit. Subsequently, the proteins were separated using 10% SDS polyacrylamide gel electrophoresis and then transferred onto a PVDF membrane. The membrane was blocked using 5% nonfat milk for 2 h at 25˚C. Subsequently, primary antibodies (TFAP2A at a dilution of 1:5,000; GAPDH at a dilution of 1:50,000) overnight at 4˚C, along with their corresponding secondary antibodies (at a dilution of 1:1,000) at 37˚C for 1 h were incubated separately. For the purpose of protein normalization, GAPDH was employed as a reference. The protein signals were detected using an ECL kit and quantified with Alpha Innotech software version 6.0 (Alpha Innotech Corporation).

Biochemical tests. The whole blood samples from mouse eyeballs were maintained at ambient temperature for 2 h, followed by centrifugation at a force of 1,000 x g for a 20 min at 4˚C. To determine the serum levels of TC, HDL-C, and LDL-C, commercially available kits were employed in conjunction

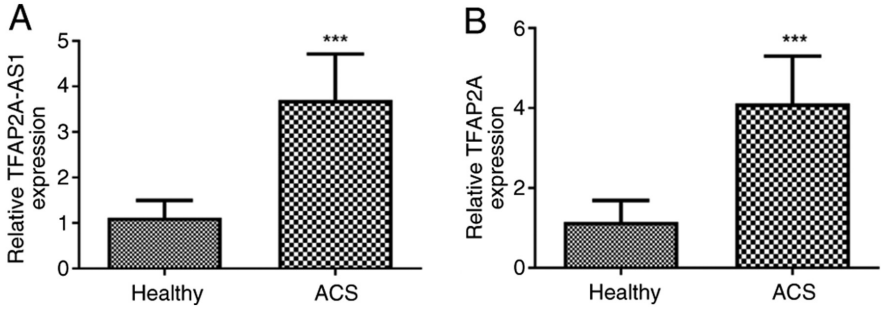

Figure 1. Serum from patients with ACS exhibits elevated expression levels of TFAP2A-AS1 and TFAP2A. The expression of (A) TFAP2A-AS1 and (B) TFAP2A in patients with ACS and healthy individuals was detected by reverse transcription-quantitative PCR. ***P<0.001 vs. Healthy. ACS, acute coronary syndrome; TFAP2A, transcription factor AP-2α.

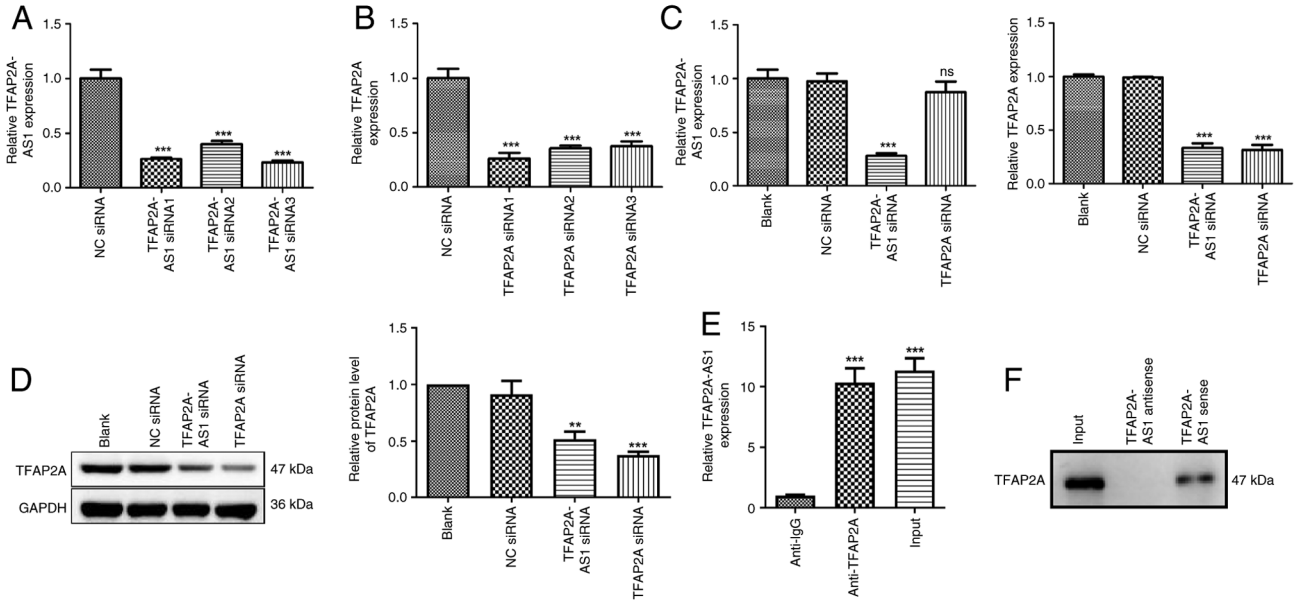

Figure 2. Silencing of TFAP2A-AS1 suppresses TFAP2A expression. (A) The expression of TFAP2A-AS1 in HCAECs after transfection with TFAP2A-AS1 siRNA1/2/3 or NC siRNA was detected by RT-qPCR. ***P<0.001 vs. NC siRNA. (B) The expression of TFAP2A in HCAECs after transfection with TFAP2A siRNA1/2/3 or NC siRNA was detected by RT-qPCR. ***P<0.001 vs. NC siRNA. (C) The expression of TFAP2A-AS1 and TFAP2A in HCAECs after transfection with TFAP2A-AS1 siRNA, TFAP2A siRNA or NC siRNA was detected by RT-qPCR. ***P<0.001 vs. NC siRNA. (D) The protein levels of TFAP2A in HCAECs after transfection with TFAP2A-AS1 siRNA, TFAP2A siRNA or NC siRNA were determined using western blotting. **P<0.01 and ***P<0.001 vs. NC siRNA. (E) RIP assay demonstrated an enrichment of TFAP2A-AS1. ***P<0.001 vs. anti-IgG. (F) RNA pull-down assay showed that TFAP2A interacting with biotin-labeled TFAP2A-AS1 was higher than that with the antisense of TFAP2A-AS1 group. TFAP2A, transcription factor AP-2α; HCAECs, human coronary artery endothelial cells; siRNA, small interfering RNA; NC, negative control; RT-qPCR, reverse transcription-quantitative PCR; RIP, RNA immunoprecipitation; ns, no significance.

with an automated bioanalysis system (Gallery Plus Discrete Analyzer; Thermo Fisher Scientific, Inc.).

H&E staining. The myocardial tissues of mice were subjected to fixation (4% paraformaldehyde at 25˚C for 12 h), deparaffinization, and hydration prior to embedding in paraffin. Subsequently, they were sectioned into slices with a thickness of 4 μm. The sections underwent a 3-min H&E staining process at 25˚C. Following the application of neutral gum for mounting, the images were captured using a Leica light microscope.

Statistical analysis. *In vitro* experiments were performed in triplicate, and each experiment was repeated 3 times. *In vivo* experiments were performed using six mice per group. The differences between two groups were evaluated using unpaired Student's t-test. To assess variations among multiple groups, a one-way ANOVA followed by Tukey's post hoc multiple comparisons test was utilized. Data analysis was performed using SPSS software version 22.0 (Dotmatics). The data were presented as the mean ± standard deviation, and P<0.05 was considered to indicate a statistically significant difference.

Results

Serum from patients with ACS exhibits elevated expression of TFAP2A-AS1 and TFAP2A. After obtaining the necessary consent from the participants, venous blood samples were collected from individuals diagnosed with ACS. Subsequently, centrifugation was conducted to obtain serum samples, and then the expression levels of TFAP2A-AS1 and TFAP2A were determined using RT-qPCR. The findings, as depicted in

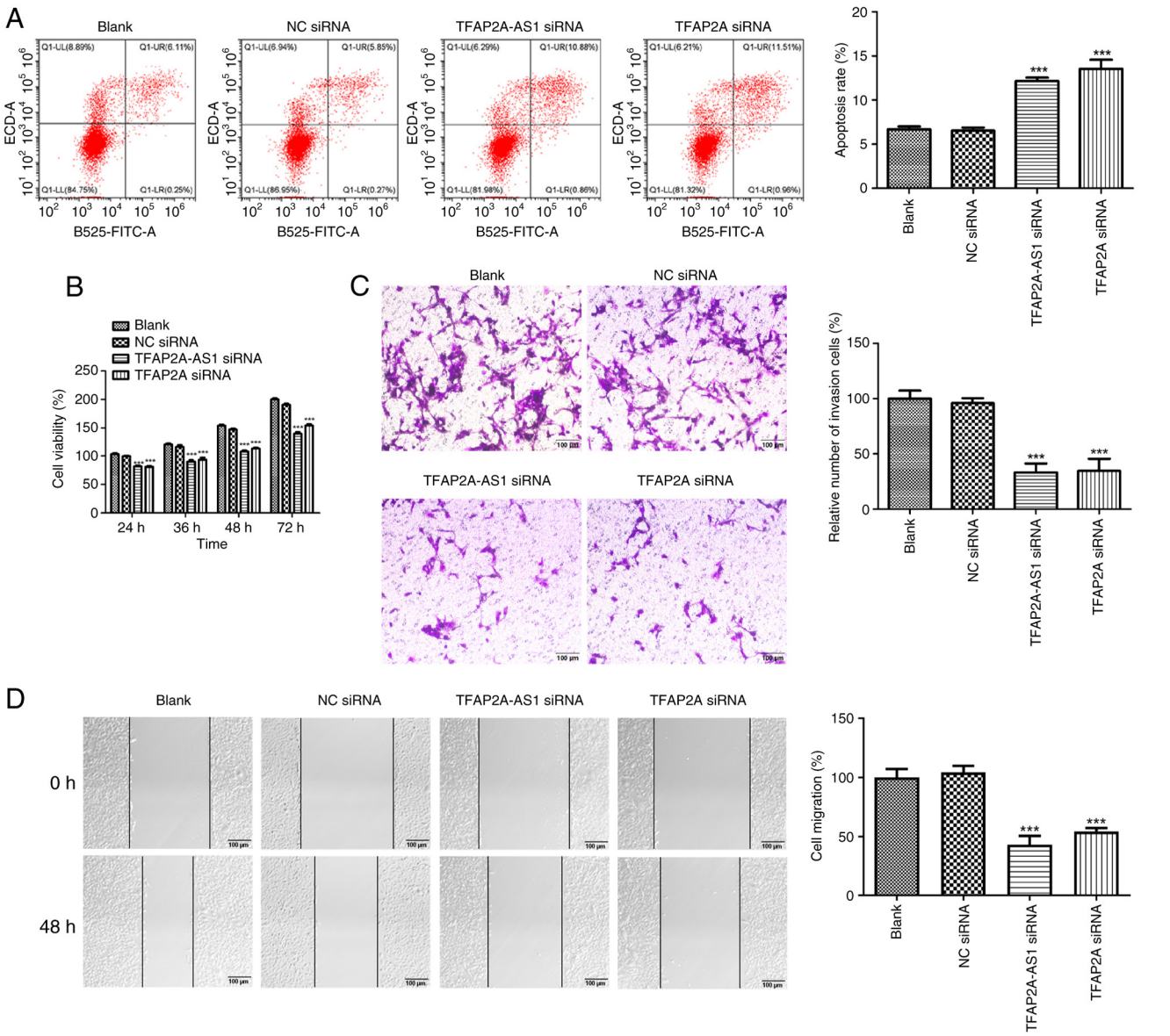

Figure 3. Silencing of TFAP2A-AS1 and TFAP2A suppresses the proliferative, migratory, and invasive capacities while enhancing the apoptotic rate of HCAECs. (A) The apoptosis rate, (B) viability, (C) invasion and (D) migration of HCAECs transfected TFAP2A-AS1 siRNA, TFAP2A siRNA or NC siRNA was assessed by flow cytometric analysis, Counting Kit-8 assay, Transwell invasion assay and wound healing assay, respectively. Scale bar, 100 μm. ***P<0.001 vs. NC siRNA. TFAP2A, transcription factor AP-2α; HCAECs, human coronary artery endothelial cells; siRNA, small interfering RNA; NC, negative control.

Fig. 1A, revealed a significant upregulation of TFAP2A-AS1 expression in patients with ACS compared with that observed in healthy individuals (P<0.001; Fig. 1B). Similarly, elevated levels of TFAP2A were also detected in patients with ACS when compared with controls without any health issues (P<0.001; Fig. 1B).

Silencing of TFAP2A-AS1 suppresses TFAP2A expression. To investigate the roles of TFAP2A-AS1 and TFAP2A in the progression of ACS *in vitro*, gene silencing techniques were initially employed to downregulate the expression levels of either TFAP2A-AS1 or TFAP2A in HCAECs. As illustrated in Fig. 2A, the HCAECs were transfected with TFAP2A-AS1 siRNA1, TFAP2A-AS1 siRNA2, and TFAP2A-AS1 siRNA3 individually. It was revealed that the expression level of TFAP2A-AS1 was significantly decreased following transfection (P<0.001). The selection of TFAP2A-AS1 siRNA3 for subsequent experiments was based on its relatively high silencing efficiency. Similarly, TFAP2A siRNA transfection also significantly inhibited TFAP2A expression, and TFAP2A siRNA1 was selected for the subsequent experiments (P<0.001; Fig. 2B). The regulatory associations between TFAP2A-AS1 and TFAP2A were then determined. The results of RT-qPCR and western blotting demonstrated that transfection of TFAP2A siRNA did not affect TFAP2A-AS1 expression, while transfection of TFAP2A-AS1 siRNA markedly decreased the mRNA expression and protein level of TFAP2A (P<0.01; Fig. 2C and D). The findings indicated that TFAP2A-AS1 possesses the capability to regulate the expression of TFAP2A; however, the converse does not hold true. A RIP assay was performed to confirm the functional interaction between TFAP2A-AS1 and TFAP2A. RNA from RIP assays using an antibody against TFAP2A was subjected to qPCR analysis, which demonstrated an enrichment of TFAP2A-AS1

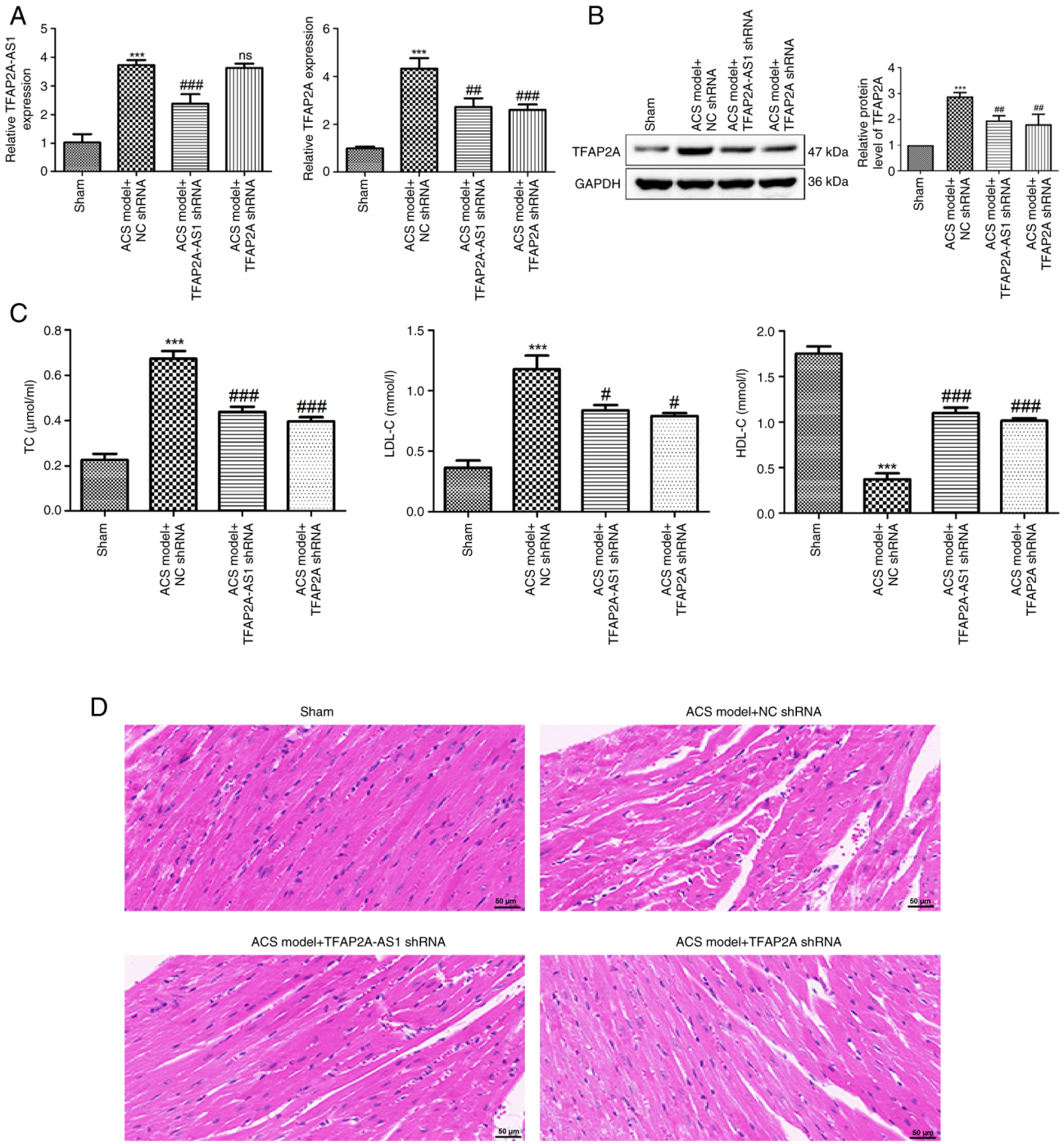

Figure 4. Knockdown of TFAP2A-AS1 and TFAP2A leads to a reduction in serum lipid levels and an improvement in myocardial injury in an ACS mouse model. (A) The expression of TFAP2A-AS1 and TFAP2A in ACS mice after injection of TFAP2A-AS1 shRNA, TFAP2A shRNA or NC shRNA was detected by reverse transcription-quantitative PCR. (B) The protein levels of TFAP2A in ACS mice after injection of TFAP2A-AS1 shRNA, TFAP2A shRNA or NC shRNA were determined using western blotting. (C) The levels of TC, LDL-C and HDL-C in ACS mice after injection of TFAP2A-AS1 shRNA, TFAP2A shRNA or NC shRNA were determined using biochemical tests. (D) Hematoxylin and eosin staining was performed to observe the pathological condition of myocardial tissues in different groups. Scale bar, 50 μm. ***P<0.001 vs. sham; $^{\#}$P<0.05, $^{\#\#}$P<0.01, and $^{\#\#\#}$P<0.001 vs. the ACS model + NC shRNA. TFAP2A, transcription factor AP-2α; ACS, acute coronary syndrome; shRNA, short hairpin RNA; ns, no significance.

(P<0.001; Fig. 2E). Next, whether TFAP2A-AS1 interacted with TFAP2A protein was examined using an RNA pull-down assay, and it was revealed that the expression level of TFAP2A interacting with biotin-labeled TFAP2A-AS1 was higher than that with the antisense TFAP2A-AS1 group (Fig. 2F). These data suggested the interaction between TFAP2A-AS1 and TFAP2A protein.

Silencing of TFAP2A-AS1 and TFAP2A inhibits the proliferative, migratory, and invasive capacities while enhancing the apoptotic rate of HCAECs. The flow cytometric analysis showed that transfection of both TFAP2A-AS1 siRNA and TFAP2A siRNA significantly increased the apoptosis rate of HCAECs (P<0.001; Fig. 3A). Starting from 24 h, the viability of HCAECs was significantly reduced following the silencing

TFAP2A-AS1 or TFAP2A (P<0.001; Fig. 3B). Additionally, the effects of TFAP2A-AS1 and TFAP2A on the invasive and migratory capacities of HCAECs were also assessed. The relative number of invasive cells was significantly decreased in the TFAP2A-AS1 siRNA and TFAP2A siRNA groups compared with those in the NC siRNA group, as demonstrated in Fig. 3C (P<0.001). Similar patterns were observed in the effects of TFAP2A-AS1 siRNA and TFAP2A siRNA on cell migration (P<0.001; Fig. 3D).

Knockdown of TFAP2A-AS1 and TFAP2A leads to a decrease in the serum lipid levels and an improvement in myocardial injury in a mouse model of ACS. A mouse model of ACS was established in the present study. As demonstrated in Fig. 4A, the expression of TFAP2A-AS1 and TFAP2A was significantly increased in mice with ACS (P<0.001). However, their expression levels were reduced after injection of TFAP2A-AS1 shRNA and TFAP2A shRNA, respectively (P<0.001). Notably, injection of TFAP2A shRNA did not affect the expression of TFAP2A-AS1, while injection of TFAP2A-AS1 shRNA significantly decreased the mRNA expression of TFAP2A in mice with ACS (P<0.01). Moreover, similar patterns were observed for the protein level of TFAP2A (P<0.01; Fig. 4B). Furthermore, it was revealed that compared with the sham group, the serum levels of TC and LDL-C were significantly elevated in a mouse model of ACS (P<0.001; Fig. 4C), while the levels of HDL-C were significantly decreased (P<0.001). Notably, the intramyocardial injection of both TFAP2A-AS1 shRNA and TFAP2A shRNA not only led to a reduction in the levels of TC and LDL-C (P<0.05), but also resulted in increased levels of HDL-C (P<0.001) in mice with ACS. Subsequently, heart tissues from mice across various groups were collected for the purpose of pathological examination. As depicted in Fig. 4D, cardiomyocytes from the sham group exhibited a normal morphology characterized by a well-organized arrangement and an absence of breaks. By contrast, cardiomyocytes derived from the ACS mice displayed signs of swelling and thickening, accompanied by irregular morphology and disordered arrangement. Following intramyocardial injection of both TFPAF-A21 shRNA and TFAF-A21 shRNA, a significant improvement in the morphology and arrangement of cardiomyocytes was observed.

Discussion

Despite significant advancements in the diagnosis and treatment of ACS, CVDs remain the leading cause of death globally. Low- and middle-income countries bear a considerable burden, with ~7 million deaths and 129 million cases of disability reported annually (17-19). Furthermore, despite a significant decline in mortality rates associated with ACS, it is still estimated that ~40% of patients will succumb to death within five years following a coronary event. The risk of fatality increases 5 to 6-fold in individuals who experience recurrent events (20,21). The economic impact associated with ACS is also substantial; with each patient in the U.S. incurring an estimated annual cost ranging from $22,528 to $32,345 primarily due to hospitalizations (22). Consequently, ACS not only imposes a significant burden on patients but also affects society at large. Therefore, there is an urgent need to explore more effective treatment options for this condition.

Most research on lncRNA TFAP2A-AS1 primarily focuses on its role in cancer. Aberrant expression of TFAP2A-AS1 has been shown to influence the occurrence and development of multiple human cancers, including GC, BC, NSCLC and OSCC (11-14). In the present study, the dysregulation of TFAP2A-AS1 was also observed in both patients with ACS and corresponding mouse models, suggesting that TFAP2A-AS1 may be significantly associated with the progression of ACS. The significance of endothelial cells in the pathogenesis of ACS should not be underestimated. The pathology of ACS represents a complex and multifaceted process, with plaque rupture identified as one of its primary triggers (3,23). Following a myocardial infarction, significant alterations occur in the behavior of endothelial cells, which are crucial for angiogenesis. Consequently, the abnormal proliferation, migration and invasion of these endothelial cells post-myocardial infarction may potentially contribute to plaque instability and erosion, ultimately leading to the onset and development of ACS (24,25). In the present study, it was demonstated that knockdown of TFAP2A-AS1 not only significantly suppressed the proliferative, invasive and migrated potentials of HCAECs, but also markedly increased the apoptosis rate. Furthermore, previous studies have reported that elevated levels of TC and LDL-C are associated with endothelial dysfunction (26,27). Based on the findings of the present study which demonstrated that silencing of TFAP2A-AS1 effectively inhibited the aberrant proliferation, invasion, and migration of HCAECs, it is reasonable to propose that the downregulation of TFAP2A-AS1 may play a pivotal role in regulating blood lipid levels. In the animal experiments, as anticipated, a significant reduction in the levels of TC and LDL-C, accompanied by an elevation in the levels of HDL-C were observed upon the injection of TFAP2A-AS1 shRNA in mice with ACS. The aforementioned results indicated that the downregulation of TFAP2A-AS1 may play a crucial role in the regulation of endothelial dysfunction. Moreover, the myocardial injury symptoms observed in ACS mice were significantly ameliorated following the injection of TFAP2A-AS1 shRNA. Therefore, the findings indicated that the absence of TFAP2A-AS1 may confer a beneficial effect on mitigating the progression of ACS.

TFAP2A, a member of the AP-2 family, has been identified as a transcription factor involved in various aspects of development (28). In branchio-oculo-facial syndrome, a rare autosomal-dominant disorder characterized by cleft palate and craniofacial abnormalities, a deletion in the TFAP2A gene has been observed (29). Additionally, studies have shown that the expression of TFAP2A is upregulated and functions as an oncogene in the progression of various cancers, including cervical cancer, gallbladder carcinoma, and ovarian cancer (30-32). Moreover, TFAP2A is essential for cardiac morphogenesis specifically during outflow tract formation and cardiac septation by regulating cell proliferation and terminal differentiation (33,34). It was therefore hypothesized that TFAP2A may also play a crucial role in ACS. In the present study, an increased expression of TFAP2A in both patients with ACS and a mouse model was observed Moreover, it was also demonstrated that the knockdown of TFAP2A could modulate endothelial dysfunction by inhibiting blood lipid levels in ACS mice, as well as suppressing the aberrant

proliferation, migration and invasion of HCAECs. All these results supported our hypothesis that TFAP2A is associated with the progression of ACS. Additionally, a recent study by Yang *et al* (35) demonstrated that the expression levels of both TFAP2A-AS1 and TFAP2A were upregulated in OSCC, exhibiting a positive correlation between their expression levels. This suggested that TFAP2A-AS1 can interact with TFAP2A to affect OSCC progression. Based on the observed effects of TFAP2A-AS1 and TFAP2A on HCAECs and mouse models, a potential association between TFAP2A-AS1 and TFAP2A in the progression of ACS was postulated. The findings demonstrated that knockdown of TFAP2A-AS1 led to decreased expression of TFAP2A, while no reciprocal effect was observed for TFAP2A on the expression of TFAP2A-AS1. In addition, the RIP and RNA pull-down assays further verified the interaction of TFAP2A-AS1 with TFAP2A. These results suggest a positive regulatory role for TFAP2A-AS1 in modulating the expression of TFAP2A. Consequently, the present study concludes that the silencing of TFAP2A-AS1 may impede the progression of ACS by inhibiting the expression of TFAP2.

Some limitations that must be acknowledged in this study are as follows: Firstly, confirming whether TFAP2A-AS1 regulates TFAP2A expression in a post-transcriptional manner may require a more rigorous approach. Secondly, the sample size of patients was relatively limited, and increasing the sample size would provide more robust data and enhance the statistical power of the findings. Thirdly, the study was conducted on a specific population in Wenzhou, China. Expanding the research to include diverse populations in China, will be considered in future studies.

In summary, the present research demonstrated that TFAP2A-AS1 acts as a pathogenic lncRNA in ACS. The suppression of TFAP2A-AS1 led to a significant decrease in TFAP2A expression, thereby hindering the progression of ACS through the regulation of endothelial dysfunction. This newly identified regulatory axis may represent a potential therapeutic target for the treatment of ACS.

Acknowledgements

Not available.

Funding

The present study was supported by Wenzhou Municipal Science and Technology Plan Project (grant no. Y20210160).

Availability of data and materials

The data are available from the corresponding author on reasonable request.

Authors' contributions

HC and SHu made substantial contributions to the conception and design of the study. SHu, FG, FY, BY, and SHa made substantial contributions to the acquisition, analysis and interpretation of data for the study. SHu drafted the manuscript. SHu, FG, FY, BY, SHa, and HC revised the manuscript critically for important intellectual content. SHu, FG, FY, BY, SHa, and HC confirm the authenticity of all the raw data. All authors read and approved the final version of the manuscript and agree to be to be accountable for all aspects of the research in ensuring that the accuracy or integrity of any part of the work are appropriately investigated and resolved.

Ethics approval and consent to participate

The patients/participants provided their written informed consent to participate in this study. The human study was conducted according to the guidelines of the Declaration of Helsinki and approved (approval no. KY-2021053) by the Ethics Committee of Wenzhou People's Hospital (Wenzhou, China). Animal experiments were conducted in compliance with the Guidelines for the Use of Laboratory Animals and approved (approval no. xmsq2022-1230) by the Ethics Committee of the First Affiliated Hospital of Wenzhou Medical University (Wenzhou, China).

Patient consent for publication

Not applicable.

Competing interests

The authors declare that they have no competing interests.

References

1. WHO CVD Risk Chart Working Group: World Health Organization cardiovascular disease risk charts: Revised models to estimate risk in 21 global regions. Lancet Glob Health 7: e1332-e1345, 2019.
2. Knuuti J, Wijns W, Saraste A, Capodanno D, Barbato E, Funck-Brentano C, Prescott E, Storey RF, Deaton C, Cuisset T, *et al*: 2019 ESC guidelines for the diagnosis and management of chronic coronary syndromes. Eur Heart J 41: 407-477, 2020.
3. Collet JP, Thiele H, Barbato E, Barthélémy O, Bauersachs J, Bhatt DL, Dendale P, Dorobantu M, Edvardsen T, Folliguet T, *et al*: 2020 ESC guidelines for the management of acute coronary syndromes in patients presenting without persistent ST-segment elevation. Eur Heart J 42: 1289-1367, 2021.
4. Kaul P, Ezekowitz JA, Armstrong PW, Leung BK, Savu A, Welsh RC, Quan H, Knudtson ML and McAlister FA: Incidence of heart failure and mortality after acute coronary syndromes. Am Heart J 165: 379-385.e2, 2013.
5. McKnight AH, Katzenberger DR and Britnell SR: Colchicine in acute coronary syndrome: A systematic review. Ann Pharmacother 55: 187-197, 2021.
6. Smith JN, Negrelli JM, Manek MB, Hawes EM and Viera AJ: Diagnosis and management of acute coronary syndrome: An evidence-based update. J Am Board Fam Med 28: 283-293, 2015.
7. Wang L and Jin Y: Noncoding RNAs as biomarkers for acute coronary syndrome. Biomed Res Int 2020: 3298696, 2020.
8. Chen H, Huang S, Guan F, Han S, Ye F, Li X and You L: Targeting circulating lncRNA ENST00000538705.1 relieves acute coronary syndrome via modulating ALOX15. Dis Markers 2022: 8208471, 2022.
9. Barbalata T, Niculescu LS, Stancu CS, Pinet F and Sima AV: Elevated levels of circulating lncRNAs LIPCAR and MALAT1 predict an unfavorable outcome in acute coronary syndrome patients. Int J Mol Sci 24: 12076, 2023.
10. Chen L and Huang Y: High expression of lncRNA PELATON serves as a risk factor for the incidence and prognosis of acute coronary syndrome. Sci Rep 12: 8030, 2022.
11. Zhao X, Chen L, Wu J, You J, Hong Q and Ye F: Transcription factor KLF15 inhibits the proliferation and migration of gastric cancer cells via regulating the TFAP2A-AS1/NISCH axis. Biol Direct 16: 21, 2021.

12. Zhou B, Guo H and Tang J: Long non-coding RNA TFAP2A-AS1 inhibits cell proliferation and invasion in breast cancer via miR-933/SMAD2. Med Sci Monit 25: 1242-1253, 2019.
13. Zhang Y, Ma L, Zhang T, Li P, Xu J and Wang Z: Long noncoding RNA TFAP2A-AS1 exerts promotive effects in non-small cell lung cancer progression via controlling the microRNA-548a-3p/CDK4 axis as a competitive endogenous RNA. Oncol Res 29: 129-139, 2022.
14. Jie G, Peng S, Cui Z, He C, Feng X and Yang K: Long non-coding RNA TFAP2A-AS1 plays an important role in oral squamous cell carcinoma: Research includes bioinformatics analysis and experiments. BMC Oral Health 22: 160, 2022.
15. Luo XY, Zhu XQ, Li Y, Wang XB, Yin W, Ge YS and Ji WM: MicroRNA-150 restores endothelial cell function and attenuates vascular remodeling by targeting PTX3 through the NF-κB signaling pathway in mice with acute coronary syndrome. Cell Biol Int 42: 1170-1181, 2018.
16. Livak KJ and Schmittgen TD: Analysis of relative gene expression data using real-time quantitative PCR and the 2(-Delta Delta C(T)) method. Methods 25: 402-408, 2001.
17. Vedanthan R, Seligman B and Fuster V: Global perspective on acute coronary syndrome: A burden on the young and poor. Circ Res 114: 1959-1975, 2014.
18. Moran AE, Oliver JT, Mirzaie M, Forouzanfar MH, Chilov M, Anderson L, Morrison JL, Khan A, Zhang N, Haynes N, *et al*: Assessing the global burden of ischemic heart disease: Part 1: Methods for a systematic review of the global epidemiology of ischemic heart disease in 1990 and 2010. Glob Heart 7: 315-329, 2012.
19. Forouzanfar MH, Moran AE, Flaxman AD, Roth G, Mensah GA, Ezzati M, Naghavi M and Murray CJ: Assessing the global burden of ischemic heart disease, part 2: Analytic methods and estimates of the global epidemiology of ischemic heart disease in 2010. Glob Heart 7: 331-342, 2012.
20. Rogers WJ, Canto JG, Lambrew CT, Tiefenbrunn AJ, Kinkaid B, Shoultz DA, Frederick PD and Every N: Temporal trends in the treatment of over 1.5 million patients with myocardial infarction in the US from 1990 through 1999: The national registry of myocardial infarction 1, 2 and 3. J Am Coll Cardiol 36: 2056-2063, 2000.
21. Thom T, Haase N, Rosamond W, Howard VJ, Rumsfeld J, Manolio T, Zheng ZJ, Flegal K, O'Donnell C, Kittner S, *et al*: Heart disease and stroke statistics-2006 update: A report from the American heart association statistics committee and stroke statistics subcommittee. Circulation 113: e85-e151, 2006.
22. Menzin J, Wygant G, Hauch O, Jackel J and Friedman M: One-year costs of ischemic heart disease among patients with acute coronary syndromes: Findings from a multi-employer claims database. Curr Med Res Opin 24: 461-468, 2008.
23. Libby P and Pasterkamp G: Requiem for the 'vulnerable plaque'. Eur Heart J 36: 2984-2987, 2015.
24. Bonetti PO, Lerman LO and Lerman A: Endothelial dysfunction: A marker of atherosclerotic risk. Arterioscler Thromb Vasc Biol 23: 168-175, 2003.
25. Zhu F, Wang Q, Guo C, Wang X, Cao X, Shi Y, Gao F, Ma C and Zhang L: IL-17 induces apoptosis of vascular endothelial cells: A potential mechanism for human acute coronary syndrome. Clin Immunol 141: 152-160, 2011.
26. Stein RA: Endothelial dysfunction, erectile dysfunction, and coronary heart disease: The pathophysiologic and clinical linkage. Rev Urol 5 (Suppl 7): S21-S27, 2003.
27. Ling L, Zhao SP, Gao M, Zhou QC, Li YL and Xia B: Vitamin C preserves endothelial function in patients with coronary heart disease after a high-fat meal. Clin Cardiol 25: 219-224, 2002.
28. Yang YL and Zhao LY: AP-2 family of transcription factors: Critical regulators of human development and cancer. J Cancer Treat Diagn 5: 1-4, 2021.
29. Gestri G, Osborne RJ, Wyatt AW, Gerrelli D, Gribble S, Stewart H, Fryer A, Bunyan DJ, Prescott K, Collin JR, *et al*: Reduced TFAP2A function causes variable optic fissure closure and retinal defects and sensitizes eye development to mutations in other morphogenetic regulators. Hum Genet 126: 791-803, 2009.
30. Zhang P, Hou Q and Yue Q: MiR-204-5p/TFAP2A feedback loop positively regulates the proliferation, migration, invasion and EMT process in cervical cancer. Cancer Biomark 28: 381-390, 2020.
31. Huang HX, Yang G, Yang Y, Yan J, Tang XY and Pan Q: TFAP2A is a novel regulator that modulates ferroptosis in gallbladder carcinoma cells via the Nrf2 signalling axis. Eur Rev Med Pharmacol Sci 24: 4745-4755, 2020.
32. Xu H, Wang L and Jiang X: Silencing of lncRNA DLEU1 inhibits tumorigenesis of ovarian cancer via regulating miR-429/TFAP2A axis. Mol Cell Biochem 476: 1051-1061, 2021.
33. Hutson MR and Kirby ML: Model systems for the study of heart development and disease. Cardiac neural crest and conotruncal malformations. Semin Cell Dev Biol 18: 101-110, 2007.
34. Hammer S, Toenjes M, Lange M, Fischer JJ, Dunkel I, Mebus S, Grimm CH, Hetzer R, Berger F and Sperling S: Characterization of TBX20 in human hearts and its regulation by TFAP2. J Cell Biochem 104: 1022-1033, 2008.
35. Yang K, Niu Y, Cui Z, Jin L, Peng S and Dong Z: Long noncoding RNA TFAP2A-AS1 promotes oral squamous cell carcinoma cell growth and movement via competitively binding miR-1297 and regulating TFAP2A expression. Mol Carcinog 61: 865-875, 2022.